Performance Aspects of Alamouti STBC for MIMO Channels Affected by Impulsive Noise

Mihaela Andrei and Viorel Nicolau

Abstract In general, wireless communications are affected by noise and by time-varying characteristics of propagation environment. Space-time block codes are an effective method to combat fading and also to provide spatial diversity. Besides fading and additive white Gaussian noise (AWGN), we considered two types of impulsive noise described by Middleton Class-A (AWCN) and symmetric α-stable (SαS) distributions. The AWCN model was used to highlight the Alamouti code diversity, compared with the situation when the channel is only affected by AWGN. Even in the presence of non-Gaussian noise, the diversity at both the reception and transmission has decreased the number of errors. Alamouti 2×2 performances for all three types of aforementioned noise are presented; the evaluation was performed considering the Bit Error Rate (BER) curves depending on signal-to-noise ratio. We have also used this code in image transmission in the presence of SαS noise. For all simulations, data was binary phase-shift keying (BPSK) modulated and the fading was Rayleigh type. Different values of the parameters that describe the noise models were considered.

Keywords Alamouti code · Alpha stable distribution · Image transmission · Impulsive noise · Middleton Class-A noise

M. Andrei (✉) · V. Nicolau
Department of Electronics and Telecommunications, "Dunarea de Jos"
University of Galati, Galati, Romania
e-mail: mihaela.andrei@ugal.ro

V. Nicolau
e-mail: viorel.nicolau@ugal.ro

P. Kulczycki et al. (eds.), *Information Technology and Computational Physics*,
Advances in Intelligent Systems and Computing 462,
DOI 10.1007/978-3-319-44260-0_8

1 Introduction

Wireless communication systems are currently in the spotlight, due to their high usage in human activities. The safety of data transmitted by such systems, on channels affected by fading, is considerably improved by using space-time block code (STBC).

STBCs ensure protection, especially at high speeds [1], and furthermore, they accomplish transmission diversity [2]. The simplest scheme is that proposed by Alamouti, with two emitting antennas [3]. This scheme is an important accomplishment in the field of communications, because it leads to good performances, in spite of having a simple decoder.

In general, any process is affected by various additive or multiplicative disturbances. In communication systems, the perturbations are additive. These are generated by various sources at different points of time and space and then are propagated through communication channels to the receivers, where they arrive as a combination of noise signals, independent or correlated. The noise that could affect the data transmission on multiple-input multiple-output (MIMO) channels can be additive white Gaussian noise or non-Gaussian (impulsive noise). Impulsive noise is an additive disturbance, independent of background noise, active at different moments of time, as very short pulses. In addition, it is a non-stationary process, whose statistical parameters may vary in time.

The main characteristic of this type of noise is high value of instantaneous power and average power ratio. As a result, impulsive noise is a significant source of errors if the pulses occur frequently and their amplitudes are much higher than background noise [4]. There are various sources that can produce non-Gaussian noise such as: automotive ignition, refrigerators, printers, microwave ovens [5], or network interference [6].

Most of the space-time block code receptors were designed for the AWGN case. That is why, in the presence of impulsive noise, their performance drops significantly, compared to the AWGN case, especially for high values of signal-to-noise ratio (SNR) [7].

Because this type of noise is often present, communications research required the development of statistical models enable to characterize it. So, in [8] Hall proposed an exogenous model, where impulsive noise is generated as a product of two independent random processes. Shao and Nikias established a symmetric stable distribution, characterized by an exponent term α and known as symmetric α-stable (SαS) distribution [9]. In many applications, for impulsive noise a canonical model is used, proposed by Middleton [4]. In this paper, Middleton Class-A and SαS distributions were considered.

In the case of MIMO communication channels with multiple receivers, the Middleton Class-A impulsive noise models are multivariable extensions of the monovariable distributions (valid for channels with a single receiver). Based on the sources of interference spatial distribution relative to the receivers, there are three types of multivariable models for Middleton Class-A impulsive noise [10]:

(a) the impulsive noises from the receivers are considered random variables, independent in space and time and evenly distributed. In this case, the noise sources are independent and each antenna receives an independent impulsive noise, generated by a monovariable probability density function (pdf). Often, the same parameters are used for all the probability densities of the random variables;
(b) the impulsive noises from the receivers are considered temporal-independent random variables, but spatially dependent and correlated between the receiving antennas. In this case, all the receiving antennas are under the influence of the same set of noise sources. Furthermore, the spatial dependency implies that the distance between the interference sources and the antennas is much greater than the distances between the antennas. As such, there is no difference between the distances from a source of interference to each antenna, and practically, the antennas receive impulsive noises that are more or less the same. The multivariable model uses a monovariable pdf, extended by the noise covariance matrix. This is the case considered in our paper.
(c) the impulsive noises from the receivers are considered temporal-independent random variables, but spatially dependent and uncorrelated.

When analyzing the behavior of communication systems in various situations and conditions, the Middleton Class-A noise model is used very often. Some of the results target wireless communication systems, like: IEEE 802.11a and IEEE 802.11b [11], other the power line communication [12]. In both cases, the system performances on a channel affected by non-Gaussian noise are significantly lower against AWGN for high signal-noise ratio (SNR) values. In a MIMO power line communication system, if the noise gets more impulsive, the Bit Error Rate (BER) increases [12]. For a MIMO system with orthogonal space-time coding (OSTBC), QPSK and 16QAM modulations, a coding gain of about 6 dB was obtained in the case of AWCN channel compared to AWGN, for low SNR [13]. If the SNR increases, the situation reverses.

In the case of the SαS distribution the situation is similar to Middleton Class-A, i.e., the non-Gaussian noise effects on MIMO systems worsen their performances. However, until now, there is no closed-form expression for the error probability [14], except for the optimal linear receivers in a single-input single-output system [15]. For space-time codes over a channel affected by fading and impulsive noise modeled SαS, [16] used Monte–Carlo simulations to compare the performance of the different decoders. The maximum-likelihood (ML) receiver leads the best performances.

This paper analyzes the Alamouti code spatial diversity on a channel affected by Middleton Class-A impulsive noise compared with an AWGN channel, for varying degrees of impulsivity: from almost Gaussian to strongly impulsive noise, given by the model parameters. It investigates the performances of Alamouti STBC with two transmitting and two receiving antennas over a channel affected impulsive noise

with SαS distribution, for a ML receiver and different values of the exponent parameter α. This type of noise was used in image transmission with the aforementioned code. In all cases, the fading was considered to be of Rayleigh type and data was BPSK modulated.

The paper is organized as follows. In Sect. 2, the impulsive noise models for the two types of noise are described and Sect. 3 presents the system model. Simulation results are presented in Sect. 4 and Sect. 5 concludes the paper.

2 Impulsive Noise Models

2.1 Symmetric-Alpha Stable (SαS) Distribution

First, we assume the SαS model to represent the impulsive noise. Some sources of impulsive noise are: underwater acoustics, low-frequency atmospheric noises and many more man-made noises [17]. Its characteristic function is [18]:

$$\varphi(t) = \exp\{j\delta\gamma - |\sigma t|^{\alpha}(1 - j\beta sign(t) \cdot w(t, \alpha))\}, \tag{1}$$

where

$$w(t, \alpha) = \begin{cases} \tan(\pi\alpha/2), \alpha \neq 1 \\ -\frac{2}{\pi}\log|t|, \alpha = 1 \end{cases} \tag{2}$$

The significance of variables in (1) is as follows [17]:

- $\alpha \in (0, 2]$—is the characteristic exponent. This parameter is the one who influences the thickness of the distribution tail. When $\alpha = 2$, the process becomes Gaussian.
- γ—represents the dispersion parameter. It is analogous to the variance from the Gaussian case.
- μ—is the location parameter and its corresponding parameter in the normal distribution is the mean.
- $\sigma \in (0, \infty)$ is the scale;
- $\beta \in [-1; 1]$—determines the distribution symmetry. Thus, if $\beta = 0$, the distribution is symmetrical about μ, if $\beta < 0$ the distribution is skewed to the left, and if $\beta > 0$—to the right.

So far, no expression has been set for the probability density function that describes the SαS distribution. However, there are two exceptions: Gaussian (if $\alpha = 2$) and Cauchy (if $\alpha = 1$) [19].

2.2 Middleton Class-A Model

The Middleton Class-A distribution statistically models the sum of electromagnetic interferences from multiple noise sources, spatially spread in an annular area around the receiver, following a Poisson distribution pattern for magnitude and uniform distribution, within the [0, 2π] interval for phase [20]. Unlike the SαS distribution, the Middleton Class-A can also include the white noise from the receiver, without changing the nature of distribution [10].

A sample of Middelton Class-A impulsive noise is given by: $n = n_g + n_i$, where n_g represents the Gaussian component and n_i is the impulsive component [21], with their variances: σ_g^2 and σ_i^2, respectively. Non-Gaussian type impulsive noise that follows the aforementioned distribution has the probability density function [22]:

$$p(n) = \sum_{m=0}^{\infty} \frac{A^m e^{-A}}{\sqrt{2\pi} m! \sigma_m} \exp\left(-\frac{n^2}{2\sigma_m^2}\right) \tag{3}$$

In the above pdf expression, m is the number of impulsive noise sources and A is the impulse index [22]. The term $m = 0$ is assigned to the Gaussian background noise component and the remaining summed components, indexed with $m > 0$, represent the impulsive noise, as a results of a sum of interferences from noise sources, spatial spread following a Poisson distribution.

Two important parameters describe the Middleton Class-A distribution: A and T. Parameter A is called impulsive index or overlapping and is the product of the average number of impulses that reach at the receiver in one second (v) from the noise sources and their average duration (T_m): $A = v \cdot T_m$ [23]. This parameter shows how impulsive is the noise at the receiver, as a result of the interference from noise sources. Depending on A value, for each moment of time, from total number of noise sources considered, only some of them will have a significant contribution in the noise of the receiver. Thus, if A has high values, it results a high density of waveform overlapping at a time and the noise is less impulsive, looking almost Gaussian (according to the Central Limit Theorem). Conversely, low values for A indicate a small overlap, so only a few sources interfere and the noise gets more impulsive. σ_m^2 is given by

$$\sigma_m^2 = \sigma^2 \cdot \frac{\frac{m}{A} + T}{1 + T}, \tag{4}$$

where $\sigma^2 = \sigma_g^2 + \sigma_i^2$ is the total noise power and

$$T = \frac{\sigma_g^2}{\sigma_i^2} \tag{5}$$

is the Gaussian factor. Analogous to parameter A, if T gets lower, the noise gets more impulsive, and if T has high values, the distribution will approach the Gaussian one.

3 STBC Model

A general scheme for a MIMO communication system, with N_T emitting and N_R receiving antennas is presented in Fig. 1. The use of this type of system significantly improves communication by providing diversity at the reception and/or emission. In this paper, we consider $N_T = 2$, $N_R = 2$, a BPSK modulator and the transmitted data are STBC encoded, which means that each antenna transmits a different version of the same input. This is an advantage because at reception it will get more signal copies, which will be affected differently by noise, interference or fading. A space-time block decoder uses all these copies to remake the transmitted data and thus, the number of errors will be lower.

The relation that describes a MIMO channel is [24]:

$$\mathbf{r} = \mathrm{H} \cdot \mathrm{x} + \mathrm{n} \tag{6}$$

where: **r** is the array of received signals, **H**—the channel matrix, **x** include the transmitted signals and **n**—the noise samples.

The channel matrix elements are the channel fading coefficients between the emitting and the receiving antennas. These can vary in time; so, at moment t, the matrix form is:

$$\mathrm{H}_t = \begin{bmatrix} h^t_{1,\,1} & h^t_{1,\,2} & \cdots & h^t_{1,\,N_T} \\ h^t_{2,\,1} & h^t_{2,\,2} & \cdots & h^t_{2,\,N_T} \\ \vdots & \vdots & \ddots & \vdots \\ h^t_{N_R,\,1} & h^t_{N_R,\,2} & \cdots & h^t_{N_R,\,N_T} \end{bmatrix} \tag{7}$$

If the channel matrix **H** varies slowly in time, being constant during the transmission of an entire frame with L symbols, but changing from frame to frame, then the channel is quasistatic or slow fading. In this case, the channel parameters vary more slowly than those of the base-band signal, and the channel coherence time,

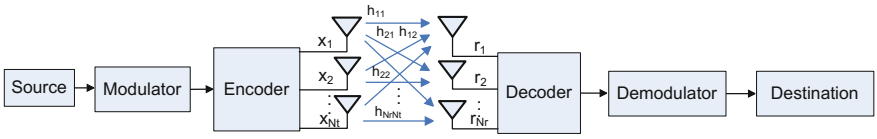

Fig. 1 The general scheme for a MIMO system with STBC encoder

denoted t_c, is bigger than the time of frame transmission, T_F: $T_F = L \cdot T < t_c$, where L is the number of symbols in the frame, and T is the transmission time of a symbol.

If the channel matrix **H** remains constant during the symbol transmission, but varies from symbol to symbol during the frame transmission, then the channel is fast fading. In this case, the coherence time is: $T < t_c < L \cdot T$.

In this study, the fading is considered to be flat and of Rayleigh type, and the coefficients to be random complex Gaussian variables, with identical distribution with zero mean and unit variance [24].

For every time moment *t*, the signal received by antenna *j* will be a linear combination of all signals, with fading and noise, and it will be given by [24]:

$$r_j^t = \sum_{i=1}^{N_T} h_{ji}^t \cdot x_i^t + n_j^t, \tag{8}$$

The scheme proposed by Alamouti has two emitting antennas and N_R receiving ones. The signals are BPSK modulated and they are transmitted as Alamouti technique: at moment *t*, the first antenna emits x_1, the second one x_2 and at the moment $t + 1$, $-x_2^*$ and x_1^*, respectively, where x^* is a complex conjugate of x [3].

According to relation (8), the signals received by antenna *j* are [24]:

$$\begin{cases} r_{j,1} = h_{j,1} \cdot x_1 + h_{j,2} \cdot x_2 + n_{j,1} \\ r_{j,2} = -h_{j,1} \cdot x_2^* + h_{j,2} \cdot x_1^* + n_{j,2} \end{cases} \tag{9}$$

The matrix form is

$$r_j = [\, r_{j,1} \quad r_{j,2} \,] = [\, h_{j,1} \quad h_{j,2} \,] \begin{bmatrix} x_1 & -x_2^* \\ x_2 & x_1^* \end{bmatrix} + [\, n_{j,1} \quad n_{j,2} \,] \tag{10}$$

The estimated symbols $\hat{x}_1$ and $\hat{x}_2$ are given using the square Euclidean distance between the received sequence and the alleged received one. Therefore, the decoder uses the maximum-likelihood algorithm. The complexity of this type of decoder depends on the number of antennas and the modulation that was used (BPSK modulated symbols are easiest to decode). As this increases, the decoding becomes more difficult.

4 Simulation Results

This part of the paper contains three subparagraphs, which present the results as follows: Alamouti code spatial diversity analysis on an AWCN channel (Sec. 4.1), the aforementioned code performances on channel affected by SαS noise (Sec. 4.2), and visual and quantitative results on image transmission using Alamouti STBC (Sec. 4.3). For all simulations, we considered a channel affected by noise (Gaussian or impulsive), Rayleigh slow fading and BPSK modulation. The ML receiver was

used. The impulsive noises, Middleton Class-A and SαS, were generated by the Interference Modeling and Mitigation Toolbox [25].

4.1 Alamouti Code Spatial Diversity Analysis on AWCN Channel

Alamouti created a space-time code with superior performances, which combats fading and ensures diversity on an AWGN channel with Rayleigh-type fading [3]. In order to highlight the benefit of this diversity on an AWCN channel also, we performed simulations for $N_R = 2$ and 4 receiving antennas and a random sequence of input data, of dimension $N = 100$ and $N = 1000$, respectively. The following situations will be considered: the transmission is affected only by the channel fading (flat fading of type Rayleigh), in which case the H matrix is considered to be perfectly known or known with uncertainty—for this case we chose o small input sequence, of size 100; fading and background noise (Gaussian) and with Middleton Class-A additional impulsive noise, respectively. The impulsive noise model parameters were varied like this: *(A, T)* = (0.1; 0.1), (0.01; 0.01). For the last scenarios, the input sequence was considered to be of size $N = 10000$.

(a) The first case considered is that when the transmission is affected only by the fading, in the absence of background noise or other sources of non-Gaussian noise. The simulations were done for a small set of input data ($N = 100$), two emitting antennas, two receiving antennas and the H matrix known at reception. In Fig. 2, we represented the symbols received by each antenna and also the estimated symbols. It can be observed that the received symbols estimation is not in the C constellation theoretical values, but within values corrected with the energy transmitted per symbol and number of transmitters. For $N_T = 2$, the estimated values of the symbols are in the $\pm 1/\sqrt{2}$ points. Even though the transmitted symbols are received with errors (caused by fading), the decoder can correct these errors, if the channel's H matrix is perfectly known.
If the H matrix is known with some uncertainty, then the estimated values will have the same uncertainty also, but the decoder will be able to correct this estimation error. We considered two situations: when the H matrix is known at reception with 20% uncertainty and 50%, respectively. The symbols' estimated values for each situation are represented in Fig. 3a and b. The symbols are no longer in the constellation points, but around them, and it can be observed that there are no decoding errors (the errors will be red).

(b) When the transmission is affected by Rayleigh fading and AWGN noise, we consider $N_R = 2$. For simulations we used a larger data set ($N = 10000$), assumed the H matrix is known and that SNR = 5, 7, 10 dB.
For SNR = 10 dB the decoding is done with a number of $N_{err} = 11$ errors. The estimated symbols' "distribution," along with the received values, is represented in Fig. 4. The red dots represent the wrongly classified points. They are

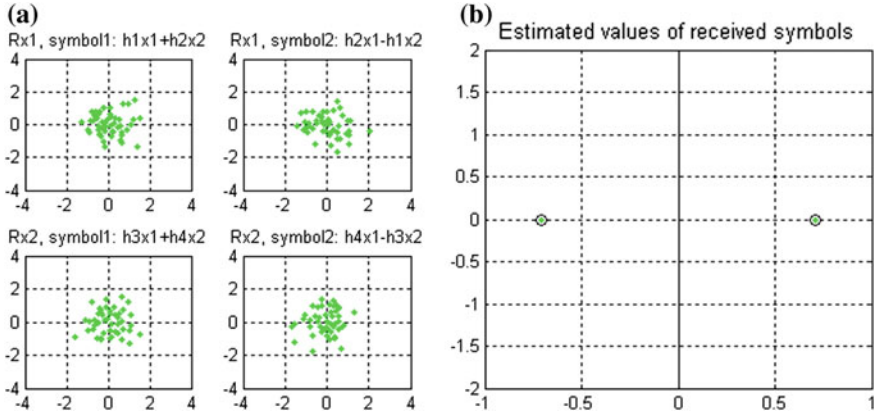

Fig. 2 Channel affected by fading and the H matrix known at reception. **a** Symbols received by each antenna; **b** estimated symbols

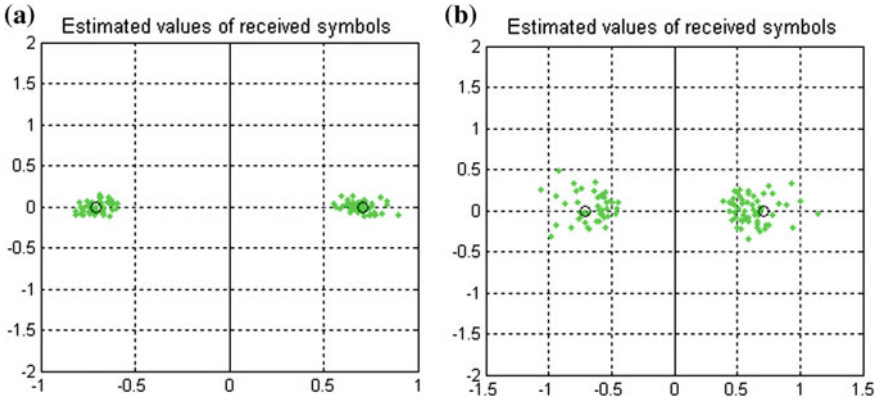

Fig. 3 Channel affected by fading and the H matrix known at reception with an uncertainty of **a** 20%; **b** 50%

placed in one of the semi-planes, left or right of the ordinate (having the real part negative or positive), but they should be in the other semi-plane.
For SNR = 7 and 5 dB, the number of errors rises N_{err} = 53 errors—at 7 dB, and 162 errors—at 5 dB, respectively, and the dots will be "distributed" like in the Figs. 5 and 6. It can be observed that most of the erroneous symbols are very close to zero.

(c) When transmission is affected by fading and AWGN noise, for N_R = 4 and H matrix known at reception, we considered the same large data set (N = 10000) and SNR = 7 dB and 5 dB, respectively.
For SNR = 7 dB, decoding is done with a number of N_{err} = 30 errors, and for SNR = 5 dB, N_{err} = 103 errors. The estimated values are represented in Fig. 7.

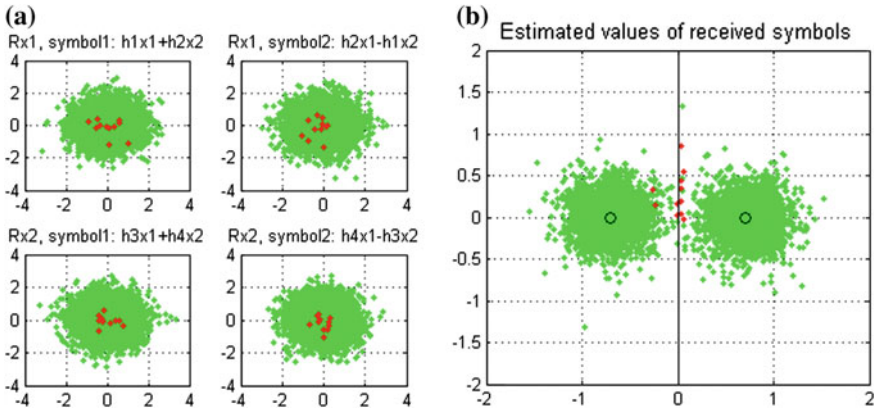

Fig. 4 Channel affected by fading and AWGN noise, $N_R = 2$. **a** Symbols received by every antenna; **b** symbols estimated at SNR = 10 dB

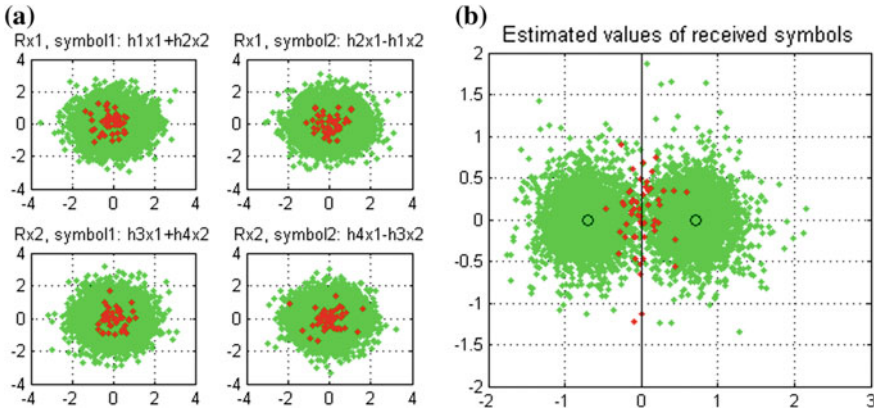

Fig. 5 Channel affected by fading and AWGN noise, $N_R = 2$. **a** Symbols received by each antenna; **b** estimated symbols, SNR = 7 dB

(d) When transmission is affected by fading, by background (Gaussian) noise and by impulsive noise, we considered $N_R = 2$, matrix H known at reception, SNR = 10 dB and *(A; T)* = (0.1; 0.1), (0.01; 0.01). The symbols distribution is given in Fig. 8. For $A = T = 0.1$, $N_{err} = 102$ errors, and for $A = 0.01$ and $T = 0.01$, the decoding is done with a number of $N_{err} = 65$ errors. A much greater spread of the wrongly classified points can be observed (compared to the AWGN case). These points, being affected by impulsive noise, have considerably passed in the opposed semi-plane. The number of errors is smaller in the case of strong impulsive noise; this has an explanation easily deductible from Fig. 8: in the case of strong impulsive noise, the impulses have greater amplitude, but they are more rare, which places the impulses far away from the

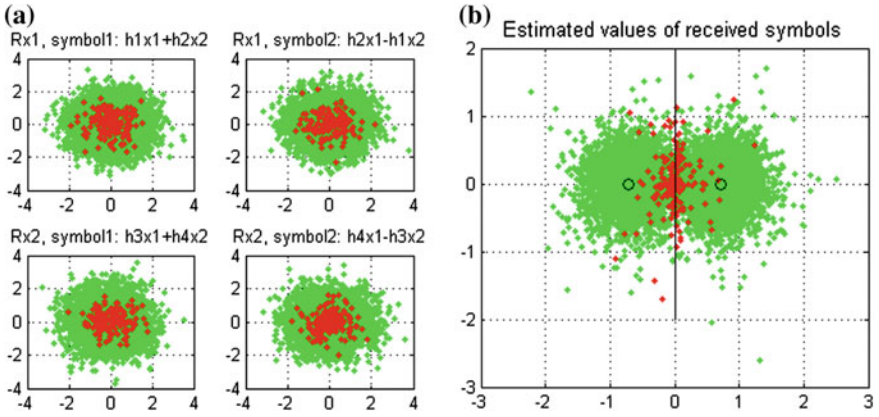

Fig. 6 Channel affected by fading and AWGN noise, $N_R = 2$. **a** Symbols received by each antenna; **b** estimated symbols, SNR = 5 dB

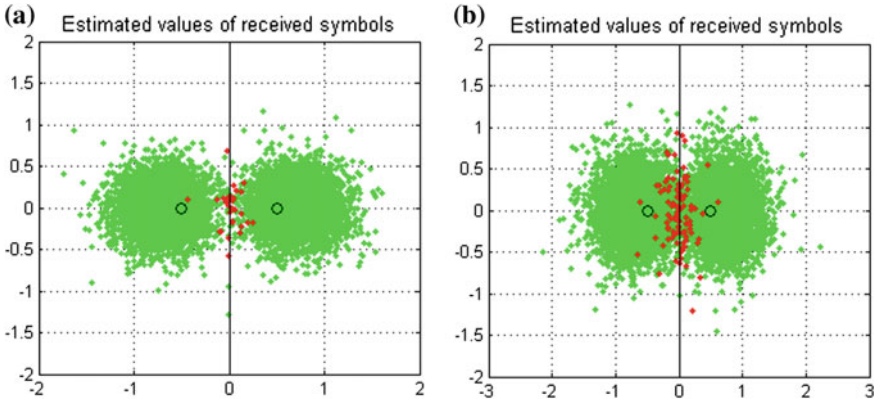

Fig. 7 Channel affected by fading and AWGN noise, $N_R = 4$. **a** SNR = 7 dB; **b** SNR = 5 dB

constellation's points. For parameters $A = T = 0.1$, the points are much closer to the constellation's ones, the erroneous ones being concentrated near 0, while for $A = T = 0.0.1$, the wrongly classified symbols are "all over the place," being less numerous, but with larger values.

(e) The last case we considered is the one when the transmission is affected by channel fading, background (Gaussian) noise and impulsive noise, but for $N_R = 4$. Assuming the H matrix is known, for SNR = 10 dB and $A = 0.1$ and $T = 0.1$, the decoding is done with a number of $N_{err} = 87$ errors, and for $A = 0.01$ and $T = 0.01$, the decoding is done with a number of $N_{err} = 52$ errors. The symbols "distribution" is represented in Fig. 9. In this case, the numbers of errors for the two parameter sets of the Middleton Class-A noise model are comparable, which means that indeed it's lucrative to have diversity

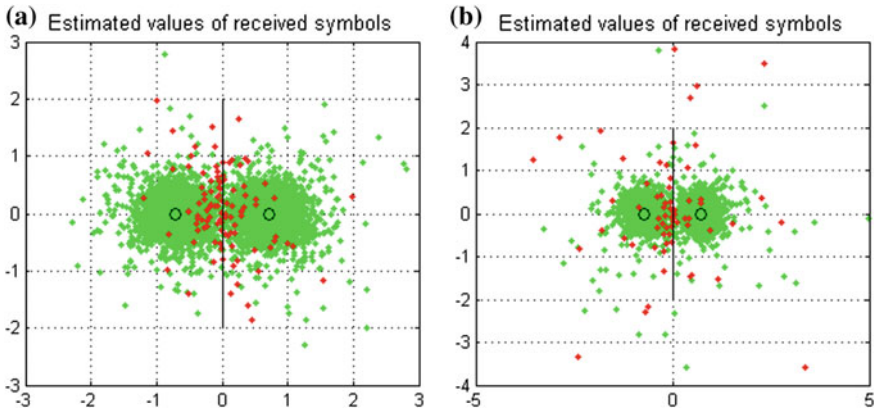

Fig. 8 AWCN channel affected by fading, $N_R = 2$, SNR = 10 dB. **a** $A = T = 0.1$; **b** $A = T = 0.01$

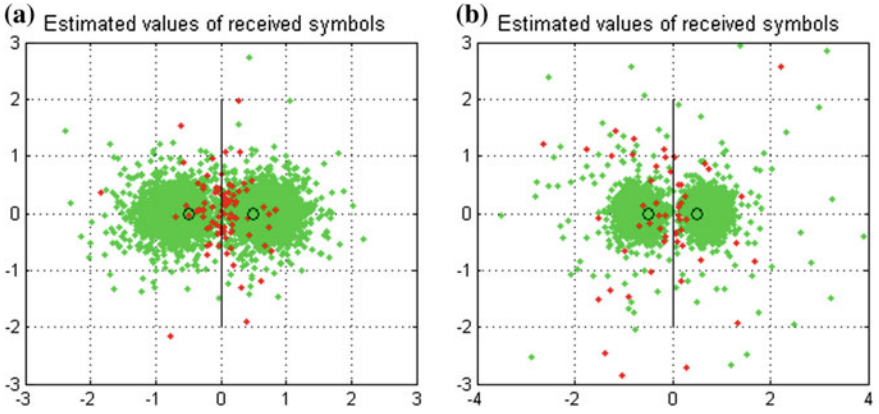

Fig. 9 AWCN channel affected by fading, $N_R = 4$, SNR = 10 dB. **a** $A = T = 0.1$; **b** $A = T = 0.01$

at reception. This situation is similar to that at point d), the number of errors being smaller for strong impulsive noise, but the impulses' high amplitude places the symbols very far from the constellation's points. Using 4 receiving antennas, at $A = T = 0.01$, we can see that the values of the estimated symbols are smaller than the ones at point d).

The results from above can be summarized in Table 1, for the AWGN channel, and Table 2, for the AWCN channel, respectively. In both cases, we considered the H matrix to be known at the receiving end, the fading to be of Rayleigh type, BPSK modulation, two emitting antennas and a data set of size N = 10000.

Table 1 Number of errors (N_{err}) for AWGN channel

SNR (dB)	N_{err}	
	Number of receiving antennas	
	2	4
5	162	103
7	53	30

Table 2 Number of errors (N_{err}) for AWCN channel

(A; T)	N_{err}	
	Number of receiving antennas	
	2	4
(0.1; 0.1)	102	87
(0.01; 0.01)	65	52

4.2 Bit Error Rate Analysis

To analyze the influence of impulsive noise on Alamouti code performances, a MIMO channel is considered with $N_T = 2$ and $N_R = 2$. The values for the model parameters are: $\alpha \in [1; 1.5; 2]$, $\beta = 0$, $\gamma = 1$, $\mu = 0$ and $\sigma = 1$. The results were compared with the cases of an AWGN channel and a Middleton Class-A (AWCN) channel with parameter $A = T = 0.01$ (highly impulsive noise) [24].

The simulation results are illustrated in Fig. 10. The impulsive noise degrades the system performances compared with AWGN. For example, for BER = 10^{-3}, the system brings a coding gain of about 3 dB when the channel is affected by Gaussian noise against SαS impulsive noise.

The poorest results are obtained in the presence of SαS noise and as α decreases, BER increases. For $\alpha = 2$, starting from SNR = 8 dB, the BER increases in case of AWCN channel. In the presence of Middleton Class-A noise, the system leads better performances for SNR values up to 3.8 dB. Beyond this point, the BER has the smallest values for AWGN channel.

4.3 Image Transmission Using Alamouti STBC

In this section, Alamouti 2 × 2 code is used for image transmission through MIMO channel. The original image is shown in Fig. 11a. It has 512 × 512 pixels with 8 bit grayscale. Figure 11b and c present the received image on AWGN and SαS ($\alpha = 1$) channels at SNR = 5 dB. The last one has the largest number of damaged pixels.

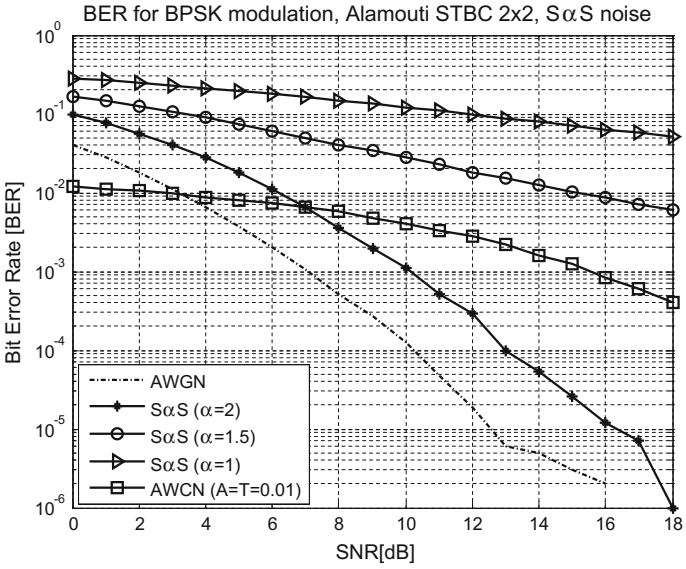

Fig. 10 BER curves for Alamouti code 2 × 2, under different type of noise

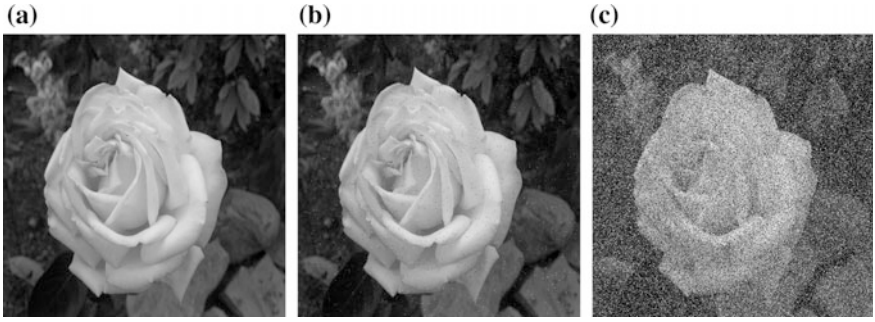

Fig. 11 **a** Original image; **b** AWGN; **c** SαS ($\alpha = 1$)

The transmitted data was BPSK modulated. The simulations were done for two SNR values: 5 and 10 dB, respectively. The image quality is assessed in terms of mean squared error (MSE) defined as:

$$MSE = \frac{1}{MN} \sum_{i=1}^{M} \sum_{j=1}^{N} [I(i,j) - \widehat{I}(i,j)]^2 \tag{11}$$

where M, N—represent the image's horizontal and vertical number of pixels, respectively; I is the original image and $\widehat{I}$ is the received image.

Table 3 Image quality metric

	SNR (dB)	Type of noise				
		AWGN	AWCN (A = T = 0.01)	SαS		
				α = 2	α = 1.5	α = 1
MSE	5	83.66	235.52	387.04	1634	4244
	10	2.37	145.37	21.78	605.43	2647

The values of MSE are collected in Table 3. The MSE values calculated for AWGN case are significantly lower than in the case of impulsive noise. It can be observed that MSE increased with the impulsive component (α). If SNR increases, the noise affects the image less, MSE having significantly lower values.

5 Conclusions

Analyzing the distribution of the estimated values of received symbols, for 2 and 4 receiving antennas, in the case of a channel affected by Gaussian and impulsive noise described by the Middleton Class-A model, it was highlighted that the spatial diversity at the receiver brings performance enhancements to the Alamouti code, on both AWGN and AWCN channels. But in the case of strongly impulsive noise ($A = T = 0.01$), the differences between the number of errors obtained for 2 and 4 receiving antennas, respectively, is not very high, while for AWGN this is cut nearly in half.

The behavior of a MIMO system, with an Alamouti 2×2 code, was investigated on a channel affected by impulsive noise and Rayleigh fading. The non-Gaussian noise was modeled with SαS type and data was BPSK modulated. The simulations were performed for different values of the exponent parameter α. The BER curves increase considerably against the AWGN channel, as α gets lower. The results were also compared with the case of AWCN channel ($A = T = 0.01$—highly impulsive). For low SNR, Middleton Class-A noise yields the best performances. The worst results, for all SNR values, are obtained for SαS noise, with $\alpha < 2$.

The image quality is strongly affected by the impulsive noise, compared to AWGN, when transmitting it on a MIMO channel. In this case, we have considered Alamouti 2×2 code, Rayleigh-type fading and SαS impulsive noise. The simulations have shown that as the noise gets more impulsive (the exponent parameter is lower), the images get more distorted (the case of $\alpha = 1$).

References

1. Tarokh, V., Seshadri, N., Calderbank, A.R.: Space–time codes for high data rate wireless communication: Performance analysis and code construction. IEEE Trans. Inf. Theory **44**(2), 744–765 (1998)
2. Vucetic, B., Yuan, J.: Space-Time Coding. Wiley, England (2003)
3. Alamouti, S.M.: A simple transmit diversity technique for wireless communications. IEEE J. Sel. Areas Comm. **16**(8), 1451–1458 (1998)
4. Middleton, D.: Statistical-physical models of electromagnetic interference. IEEE Trans. Electromagn. Compat **EMC-19**(3), 106–127 (1977)
5. Al-Dharrab, S., Uysal, M.: Cooperative diversity in the presence of impulsive noise. IEEE Trans. Wireless Commun. **8**(9), 4730–4739 (2009)
6. Win, M., Pinto, P., Shepp, L.: A mathematical theory of network interference and its applications. Proc. IEEE **97**(2), 205–230 (2009)
7. Madi, G., Sacuto, F., Vrigenau, B., Agba, B.L., Vauzelle, R., Gagnon, F.: Impact of impulsive noise from partial discharges on wireless systems performance: applications to MIMO precoders. EURASIP J. Wirel. Commun. Network. **2011**, 186 (2011)
8. Hall, H.M.: A new model for impulsive phenomena: application to atmospheric-noise communication channels. Stanford University, Technical Report, August 1966
9. Shao, M., Nikias, C.L.: On symmetric stable models for impulsive noise. University Southern California, Los Angeles, Technical Report USC-SIPI-231 (1993)
10. Chopra, A., Evans, B.L.: Join statistics of radio frequency interference in multi antenna receivers. IEEE Trans. Signal Process. **60**(7), 3588–3603 (2012)
11. Bhatti, S.A., Shan, Q., Glover, I.A., Atkinson, R., Portugues, I.E., Moore, P.J., Rutherford, R.: Impulsive noise modeling and prediction of its impact on the performance of WLAN receiver. In: 17th European Signal Processing Conference (EUSIPCO 2009), pp. 1680–1684 (2009)
12. Yoo, J., Choe, S.: Performance of space–time–frequency coding over indoor power line channels. IEEE Trans. Commun. **62**(9), 3326–3335 (2014)
13. Gong, Y., Wang, X., He, R., Pang, F.: Performance of space-time block coding under impulsive noise environment. In: Proceedings IEEE of 2nd International Conference on Advanced Computer Control, vol. 4, pp. 445–448 (2010)
14. Rajan, Tepedelenlioglu, C.: Diversity combining over Rayleigh fading channels with symmetric alpha stable noise. IEEE Trans. Wirel. Commun. **9**(9), 2968–2976 (2010)
15. Niranjayan, S., Beaulieu, N.: The BER optimal linear rake receiver for signal detection in symmetric alpha-stable noise. IEEE Trans. Commun. **57**(12), 3585–4588 (2009)
16. Lee, J., Tepedelenlioglu, C.: Space-time coding over fading channels with stable noise. IEEE Trans. Veh. Technol. **60**(7), 396–400 (2011)
17. Zha, D., Qiu, T.: Direction finding in non-Gaussian impulsive noise environments. Digit. Signal Proc. **17**, 451–465 (2007)
18. Nikias, C.L., Shao, M.: Signal Processing with Alpha-Stable Distributions and Applications. Wiley, New York (1995)
19. Gu, W., Peters, G., Clavier, L., Septier, F., Nevat, I.: Receiver study for cooperative communications in convolved additive α-stable interference plus Gaussian thermal noise. In: Ninth International Symposium on Wireless Communication Systems, pp. 451–455 (2012)
20. Middleton, D.: Non-Gaussian noise models in signal processing for telecommunications: new methods and results for class A and class B noise models. IEEE Trans. Inf. Theory **45**(4), 1129–1149 (1999)
21. Saaifan, K.A., Henkel, W.: A spatial diversity reception of binary signal transmission over rayleigh fading channels with correlated impulse noise. In: 19th International Conference on Telecommunications (ICT 2012), pp. 1–5, Jounieh, Lebanon (2012)
22. Umehara, D., Yamaguchi, H., Morihiro, Y.: Turbo decoding over impulse noise channel. In: Proceedings of IEEE ISPLC (2004)

23. Spaulding, A., Middleton, D.: Optimum reception in an impulsive interference environment-part I: coherent detection. IEEE Trans. Commun. **25**(9), 910–923 (1977)
24. Andrei, M., Trifina, L., Tarniceriu, D.: Influence of impulse noise on Alamouti code performances. Proc. Wirel. Mobile Appl. ECUMICT **2014**, 11–21 (2014)
25. Gulati, K., Nassar, M., Chopra, A., Ben Okafor, N., DeYoung, M., Aghasadeghi, N., Sujeeth, A., Evans, B.L.: Interference modeling and mitigation toolbox 1.6, for matlab. ESP Laboratory, ECE Department, University of Texas at Austin (2011)